

Top Quark Mass Measurement in the Lepton + Jets Channel Using a Matrix Element Method and *in situ* Jet Energy Calibration

T. Aaltonen,²¹ B. Álvarez González^v,⁹ S. Amerio,⁴¹ D. Amidei,³² A. Anastassov,³⁶ A. Annovi,¹⁷ J. Antos,¹² G. Apollinari,¹⁵ J.A. Appel,¹⁵ A. Apresyan,⁴⁶ T. Arisawa,⁵⁷ A. Artikov,¹³ J. Asaadi,⁵¹ W. Ashmanskas,¹⁵ B. Auerbach,⁶⁰ A. Aurisano,⁵¹ F. Azfar,⁴⁰ W. Badgett,¹⁵ A. Barbaro-Galtieri,²⁶ V.E. Barnes,⁴⁶ B.A. Barnett,²³ P. Barria^{cc},⁴⁴ P. Bartos,¹² M. Bauce^{aa},⁴¹ G. Bauer,³⁰ F. Bedeschi,⁴⁴ D. Beecher,²⁸ S. Behari,²³ G. Bellettini^{bb},⁴⁴ J. Bellinger,⁵⁹ D. Benjamin,¹⁴ A. Beretvas,¹⁵ A. Bhatti,⁴⁸ M. Binkley*,¹⁵ D. Bisello^{aa},⁴¹ I. Bizjak^{gg},²⁸ K.R. Bland,⁵ B. Blumenfeld,²³ A. Bocci,¹⁴ A. Bodek,⁴⁷ D. Bortoletto,⁴⁶ J. Boudreau,⁴⁵ A. Boveia,¹¹ B. Brau^a,¹⁵ L. Brigliadori^z,⁶ A. Brisuda,¹² C. Bromberg,³³ E. Brucken,²¹ M. Bucchiantonio^{bb},⁴⁴ J. Budagov,¹³ H.S. Budd,⁴⁷ S. Budd,²² K. Burkett,¹⁵ G. Busetto^{aa},⁴¹ P. Bussey,¹⁹ A. Buzatu,³¹ C. Calancha,²⁹ S. Camarda,⁴ M. Campanelli,³³ M. Campbell,³² F. Canelli¹²,¹⁵ A. Canepa,⁴³ B. Carls,²² D. Carlsmith,⁵⁹ R. Carosi,⁴⁴ S. Carrillo^k,¹⁶ S. Carron,¹⁵ B. Casal,⁹ M. Casarsa,¹⁵ A. Castro^z,⁶ P. Catastini,¹⁵ D. Cauz,⁵³ V. Cavaliere^{cc},⁴⁴ M. Cavalli-Sforza,⁴ A. Cerri^f,²⁶ L. Cerrito^q,²⁸ Y.C. Chen,¹ M. Chertok,⁷ G. Chiarelli,⁴⁴ G. Chlachidze,¹⁵ F. Chlebana,¹⁵ K. Cho,²⁵ D. Chokheli,¹³ J.P. Chou,²⁰ W.H. Chung,⁵⁹ Y.S. Chung,⁴⁷ C.I. Ciobanu,⁴² M.A. Ciocci^{cc},⁴⁴ A. Clark,¹⁸ G. Compostella^{aa},⁴¹ M.E. Convery,¹⁵ J. Conway,⁷ M. Corbo,⁴² M. Cordelli,¹⁷ C.A. Cox,⁷ D.J. Cox,⁷ F. Crescioli^{bb},⁴⁴ C. Cuenca Almenar,⁶⁰ J. Cuevas^v,⁹ R. Culbertson,¹⁵ D. Dagenhart,¹⁵ N. d'Ascenzo^t,⁴² M. Datta,¹⁵ P. de Barbaro,⁴⁷ S. De Cecco,⁴⁹ G. De Lorenzo,⁴ M. Dell'Orso^{bb},⁴⁴ C. Deluca,⁴ L. Demortier,⁴⁸ J. Deng^c,¹⁴ M. Deninno,⁶ F. Devoto,²¹ M. d'Errico^{aa},⁴¹ A. Di Canto^{bb},⁴⁴ B. Di Ruzza,⁴⁴ J.R. Dittmann,⁵ M. D'Onofrio,²⁷ S. Donati^{bb},⁴⁴ P. Dong,¹⁵ T. Dorigo,⁴¹ K. Ebina,⁵⁷ A. Elagin,⁵¹ A. Eppig,³² R. Erbacher,⁷ D. Errede,²² S. Errede,²² N. Ershaidat^y,⁴² R. Eusebi,⁵¹ H.C. Fang,²⁶ S. Farrington,⁴⁰ M. Feindt,²⁴ J.P. Fernandez,²⁹ C. Ferrazza^{dd},⁴⁴ R. Field,¹⁶ G. Flanagan^r,⁴⁶ R. Forrest,⁷ M.J. Frank,⁵ M. Franklin,²⁰ J.C. Freeman,¹⁵ I. Furic,¹⁶ M. Gallinaro,⁴⁸ J. Galyardt,¹⁰ J.E. Garcia,¹⁸ A.F. Garfinkel,⁴⁶ P. Garosi^{cc},⁴⁴ H. Gerberich,²² E. Gerchtein,¹⁵ S. Giagu^{ee},⁴⁹ V. Giakoumopoulou,³ P. Giannetti,⁴⁴ K. Gibson,⁴⁵ C.M. Ginsburg,¹⁵ N. Giokaris,³ P. Giromini,¹⁷ M. Giunta,⁴⁴ G. Giurgiu,²³ V. Glagolev,¹³ D. Glenzinski,¹⁵ M. Gold,³⁵ D. Goldin,⁵¹ N. Goldschmidt,¹⁶ A. Golossanov,¹⁵ G. Gomez,⁹ G. Gomez-Ceballos,³⁰ M. Goncharov,³⁰ O. González,²⁹ I. Gorelov,³⁵ A.T. Goshaw,¹⁴ K. Goulianos,⁴⁸ A. Gresele,⁴¹ S. Grinstein,⁴ C. Grosso-Pilcher,¹¹ R.C. Group,⁵⁶ J. Guimaraes da Costa,²⁰ Z. Gunay-Unalan,³³ C. Haber,²⁶ S.R. Hahn,¹⁵ E. Halkiadakis,⁵⁰ A. Hamaguchi,³⁹ J.Y. Han,⁴⁷ F. Happacher,¹⁷ K. Hara,⁵⁴ D. Hare,⁵⁰ M. Hare,⁵⁵ R.F. Harr,⁵⁸ K. Hatakeyama,⁵ C. Hays,⁴⁰ M. Heck,²⁴ J. Heinrich,⁴³ M. Herndon,⁵⁹ S. Hewamanage,⁵ D. Hidas,⁵⁰ A. Hocker,¹⁵ W. Hopkins^q,¹⁵ D. Horn,²⁴ S. Hou,¹ R.E. Hughes,³⁷ M. Hurwitz,¹¹ U. Husemann,⁶⁰ N. Hussain,³¹ M. Hussein,³³ J. Huston,³³ G. Introzzi,⁴⁴ M. Iori^{ee},⁴⁹ A. Ivanov^o,⁷ E. James,¹⁵ D. Jang,¹⁰ B. Jayatilaka,¹⁴ E.J. Jeon,²⁵ M.K. Jha,⁶ S. Jindariani,¹⁵ W. Johnson,⁷ M. Jones,⁴⁶ K.K. Joo,²⁵ S.Y. Jun,¹⁰ T.R. Junk,¹⁵ T. Kamon,⁵¹ P.E. Karchin,⁵⁸ Y. Katoⁿ,³⁹ W. Ketchum,¹¹ J. Keung,⁴³ V. Khotilovich,⁵¹ B. Kilminster,¹⁵ D.H. Kim,²⁵ H.S. Kim,²⁵ H.W. Kim,²⁵ J.E. Kim,²⁵ M.J. Kim,¹⁷ S.B. Kim,²⁵ S.H. Kim,⁵⁴ Y.K. Kim,¹¹ N. Kimura,⁵⁷ M. Kirby,¹⁵ S. Klimenko,¹⁶ K. Kondo,⁵⁷ D.J. Kong,²⁵ J. Konigsberg,¹⁶ A.V. Kotwal,¹⁴ M. Kreps,²⁴ J. Kroll,⁴³ D. Krop,¹¹ N. Krumnack^l,⁵ M. Kruse,¹⁴ V. Krutelyov^d,⁵¹ T. Kuhr,²⁴ M. Kurata,⁵⁴ S. Kwang,¹¹ A.T. Laasanen,⁴⁶ S. Lami,⁴⁴ S. Lammel,¹⁵ M. Lancaster,²⁸ R.L. Lander,⁷ K. Lannon^u,³⁷ A. Lath,⁵⁰ G. Latino^{cc},⁴⁴ I. Lazzizzera,⁴¹ T. LeCompte,² E. Lee,⁵¹ H.S. Lee,¹¹ J.S. Lee,²⁵ S.W. Lee^w,⁵¹ S. Leo^{bb},⁴⁴ S. Leone,⁴⁴ J.D. Lewis,¹⁵ C.-J. Lin,²⁶ J. Linacre,⁴⁰ M. Lindgren,¹⁵ E. Lipeles,⁴³ A. Lister,¹⁸ D.O. Litvintsev,¹⁵ C. Liu,⁴⁵ Q. Liu,⁴⁶ T. Liu,¹⁵ S. Lockwitz,⁶⁰ N.S. Lockyer,⁴³ A. Loginov,⁶⁰ D. Lucchesi^{aa},⁴¹ J. Lueck,²⁴ P. Lujan,²⁶ P. Lukens,¹⁵ G. Lungu,⁴⁸ J. Lys,²⁶ R. Lysak,¹² R. Madrak,¹⁵ K. Maeshima,¹⁵ K. Makhoul,³⁰ P. Maksimovic,²³ S. Malik,⁴⁸ G. Manca^b,²⁷ A. Manousakis-Katsikakis,³ F. Margaroli,⁴⁶ C. Marino,²⁴ M. Martínez,⁴ R. Martínez-Ballarín,²⁹ P. Mastrandrea,⁴⁹ M. Mathis,²³ M.E. Mattson,⁵⁸ P. Mazzanti,⁶ K.S. McFarland,⁴⁷ P. McIntyre,⁵¹ R. McNultyⁱ,²⁷ A. Mehta,²⁷ P. Mehtala,²¹ A. Menzione,⁴⁴ C. Mesropian,⁴⁸ T. Miao,¹⁵ D. Mietlicki,³² A. Mitra,¹ H. Miyake,⁵⁴ S. Moed,²⁰ N. Moggi,⁶ M.N. Mondragon^k,¹⁵ C.S. Moon,²⁵ R. Moore,¹⁵ M.J. Morello,¹⁵ J. Morlock,²⁴ P. Movilla Fernandez,¹⁵ A. Mukherjee,¹⁵ Th. Muller,²⁴ P. Murat,¹⁵ M. Mussini^z,⁶ J. Nachtman^m,¹⁵ Y. Nagai,⁵⁴ J. Naganoma,⁵⁷ I. Nakano,³⁸ A. Napier,⁵⁵ J. Nett,⁵⁹ C. Neu,⁵⁶ M.S. Neubauer,²² J. Nielsen^e,²⁶ L. Nodulman,² O. Norniella,²² E. Nurse,²⁸ L. Oakes,⁴⁰ S.H. Oh,¹⁴ Y.D. Oh,²⁵ I. Oksuzian,⁵⁶ T. Okusawa,³⁹ R. Orava,²¹ L. Ortolan,⁴ S. Pagan Griso^{aa},⁴¹ C. Pagliarone,⁵³ E. Palencia^f,⁹ V. Papadimitriou,¹⁵ A.A. Paramonov,² J. Patrick,¹⁵ G. Pauletta^{ff},⁵³ M. Paulini,¹⁰ C. Paus,³⁰ D.E. Pellett,⁷ A. Penzo,⁵³ T.J. Phillips,¹⁴ G. Piacentino,⁴⁴ E. Pianori,⁴³ J. Pilot,³⁷ K. Pitts,²² C. Plager,⁸ L. Pondrom,⁵⁹ K. Potamianos,⁴⁶ O. Poukhov*,¹³

F. Prokoshin^{x,13} A. Pronko,¹⁵ F. Ptohos^{h,17} E. Pueschel,¹⁰ G. Punzi^{bb,44} J. Pursley,⁵⁹ A. Rahaman,⁴⁵ V. Ramakrishnan,⁵⁹ N. Ranjan,⁴⁶ I. Redondo,²⁹ P. Renton,⁴⁰ M. Rescigno,⁴⁹ F. Rimondi^{z,6} L. Ristori^{45,15} A. Robson,¹⁹ T. Rodrigo,⁹ T. Rodriguez,⁴³ E. Rogers,²² S. Rolli,⁵⁵ R. Roser,¹⁵ M. Rossi,⁵³ F. Rubbo,¹⁵ F. Ruffini^{cc,44} A. Ruiz,⁹ J. Russ,¹⁰ V. Rusu,¹⁵ A. Safonov,⁵¹ W.K. Sakumoto,⁴⁷ L. Santi^{ff,53} L. Sartori,⁴⁴ K. Sato,⁵⁴ V. Saveliev^{t,42} A. Savoy-Navarro,⁴² P. Schlabach,¹⁵ A. Schmidt,²⁴ E.E. Schmidt,¹⁵ M.P. Schmidt^{*,60} M. Schmitt,³⁶ T. Schwarz,⁷ L. Scodellaro,⁹ A. Scribano^{cc,44} F. Scuri,⁴⁴ A. Sedov,⁴⁶ S. Seidel,³⁵ Y. Seiya,³⁹ A. Semenov,¹³ F. Sforza^{bb,44} A. Sfyrta,²² S.Z. Shalhout,⁷ T. Shears,²⁷ P.F. Shepard,⁴⁵ M. Shimojima^{s,54} S. Shiraishi,¹¹ M. Shochet,¹¹ I. Shreyber,³⁴ J. Siegrist,²⁶ A. Simonenko,¹³ P. Sinervo,³¹ A. Sissakian^{*,13} K. Sliwa,⁵⁵ J.R. Smith,⁷ F.D. Snider,¹⁵ A. Soha,¹⁵ S. Somalwar,⁵⁰ V. Sorin,⁴ P. Squillacioti,¹⁵ M. Stanitzki,⁶⁰ R. St. Denis,¹⁹ B. Stelzer,³¹ O. Stelzer-Chilton,³¹ D. Stentz,³⁶ J. Strologas,³⁵ G.L. Strycker,³² Y. Sudo,⁵⁴ A. Sukhanov,¹⁶ I. Suslov,¹³ K. Takemasa,⁵⁴ Y. Takeuchi,⁵⁴ J. Tang,¹¹ M. Tecchio,³² P.K. Teng,¹ J. Thom^{g,15} J. Thome,¹⁰ G.A. Thompson,²² E. Thomson,⁴³ P. Ttito-Guzmán,²⁹ S. Tkaczyk,¹⁵ D. Toback,⁵¹ S. Tokar,¹² K. Tollefson,³³ T. Tomura,⁵⁴ D. Tonelli,¹⁵ S. Torre,¹⁷ D. Torretta,¹⁵ P. Totaro^{ff,53} M. Trovato^{dd,44} Y. Tu,⁴³ N. Turini^{cc,44} F. Ukegawa,⁵⁴ S. Uozumi,²⁵ A. Varganov,³² E. Vataga^{dd,44} F. Vázquez^{k,16} G. Velev,¹⁵ C. Vellidis,³ M. Vidal,²⁹ I. Vila,⁹ R. Vilar,⁹ I. Volobouev,⁵² M. Vogel,³⁵ G. Volpi^{bb,44} P. Wagner,⁴³ R.L. Wagner,¹⁵ T. Wakisaka,³⁹ R. Wallny,⁸ S.M. Wang,¹ A. Warburton,³¹ D. Waters,²⁸ M. Weinberger,⁵¹ W.C. Wester III,¹⁵ B. Whitehouse,⁵⁵ D. Whiteson^{c,43} A.B. Wicklund,² E. Wicklund,¹⁵ S. Wilbur,¹¹ F. Wick,²⁴ H.H. Williams,⁴³ J.S. Wilson,³⁷ P. Wilson,¹⁵ B.L. Winer,³⁷ P. Wittich^{g,15} S. Wolbers,¹⁵ H. Wolfe,³⁷ T. Wright,³² X. Wu,¹⁸ Z. Wu,⁵ K. Yamamoto,³⁹ J. Yamaoka,¹⁴ T. Yang,¹⁵ U.K. Yang^{p,11} Y.C. Yang,²⁵ W.-M. Yao,²⁶ G.P. Yeh,¹⁵ K. Yi^{m,15} J. Yoh,¹⁵ K. Yorita,⁵⁷ T. Yoshida^{j,39} G.B. Yu,¹⁴ I. Yu,²⁵ S.S. Yu,¹⁵ J.C. Yun,¹⁵ A. Zanetti,⁵³ Y. Zeng,¹⁴ and S. Zucchelli^{z6}

(CDF Collaboration[†])

¹*Institute of Physics, Academia Sinica, Taipei, Taiwan 11529, Republic of China*

²*Argonne National Laboratory, Argonne, Illinois 60439, USA*

³*University of Athens, 157 71 Athens, Greece*

⁴*Institut de Fisica d'Altes Energies, Universitat Autònoma de Barcelona, E-08193, Bellaterra (Barcelona), Spain*

⁵*Baylor University, Waco, Texas 76798, USA*

⁶*Istituto Nazionale di Fisica Nucleare Bologna, ^zUniversity of Bologna, I-40127 Bologna, Italy*

⁷*University of California, Davis, Davis, California 95616, USA*

⁸*University of California, Los Angeles, Los Angeles, California 90024, USA*

⁹*Instituto de Fisica de Cantabria, CSIC-University of Cantabria, 39005 Santander, Spain*

¹⁰*Carnegie Mellon University, Pittsburgh, Pennsylvania 15213, USA*

¹¹*Enrico Fermi Institute, University of Chicago, Chicago, Illinois 60637, USA*

¹²*Comenius University, 842 48 Bratislava, Slovakia; Institute of Experimental Physics, 040 01 Kosice, Slovakia*

¹³*Joint Institute for Nuclear Research, RU-141980 Dubna, Russia*

¹⁴*Duke University, Durham, North Carolina 27708, USA*

¹⁵*Fermi National Accelerator Laboratory, Batavia, Illinois 60510, USA*

¹⁶*University of Florida, Gainesville, Florida 32611, USA*

¹⁷*Laboratori Nazionali di Frascati, Istituto Nazionale di Fisica Nucleare, I-00044 Frascati, Italy*

¹⁸*University of Geneva, CH-1211 Geneva 4, Switzerland*

¹⁹*Glasgow University, Glasgow G12 8QQ, United Kingdom*

²⁰*Harvard University, Cambridge, Massachusetts 02138, USA*

²¹*Division of High Energy Physics, Department of Physics, University of Helsinki and Helsinki Institute of Physics, FIN-00014, Helsinki, Finland*

²²*University of Illinois, Urbana, Illinois 61801, USA*

²³*The Johns Hopkins University, Baltimore, Maryland 21218, USA*

²⁴*Institut für Experimentelle Kernphysik, Karlsruhe Institute of Technology, D-76131 Karlsruhe, Germany*

²⁵*Center for High Energy Physics: Kyungpook National University,*

Daegu 702-701, Korea; Seoul National University, Seoul 151-742,

Korea; Sungkyunkwan University, Suwon 440-746,

Korea; Korea Institute of Science and Technology Information,

Daejeon 305-806, Korea; Chonnam National University, Gwangju 500-757,

Korea; Chonbuk National University, Jeonju 561-756, Korea

²⁶*Ernest Orlando Lawrence Berkeley National Laboratory, Berkeley, California 94720, USA*

²⁷*University of Liverpool, Liverpool L69 7ZE, United Kingdom*

²⁸*University College London, London WC1E 6BT, United Kingdom*

²⁹*Centro de Investigaciones Energeticas Medioambientales y Tecnológicas, E-28040 Madrid, Spain*

³⁰*Massachusetts Institute of Technology, Cambridge, Massachusetts 02139, USA*

- ³¹*Institute of Particle Physics: McGill University, Montréal, Québec, Canada H3A 2T8; Simon Fraser University, Burnaby, British Columbia, Canada V5A 1S6; University of Toronto, Toronto, Ontario, Canada M5S 1A7; and TRIUMF, Vancouver, British Columbia, Canada V6T 2A3*
- ³²*University of Michigan, Ann Arbor, Michigan 48109, USA*
- ³³*Michigan State University, East Lansing, Michigan 48824, USA*
- ³⁴*Institution for Theoretical and Experimental Physics, ITEP, Moscow 117259, Russia*
- ³⁵*University of New Mexico, Albuquerque, New Mexico 87131, USA*
- ³⁶*Northwestern University, Evanston, Illinois 60208, USA*
- ³⁷*The Ohio State University, Columbus, Ohio 43210, USA*
- ³⁸*Okayama University, Okayama 700-8530, Japan*
- ³⁹*Osaka City University, Osaka 588, Japan*
- ⁴⁰*University of Oxford, Oxford OX1 3RH, United Kingdom*
- ⁴¹*Istituto Nazionale di Fisica Nucleare, Sezione di Padova-Trento, ^{aa}University of Padova, I-35131 Padova, Italy*
- ⁴²*LPNHE, Université Pierre et Marie Curie/IN2P3-CNRS, UMR7585, Paris, F-75252 France*
- ⁴³*University of Pennsylvania, Philadelphia, Pennsylvania 19104, USA*
- ⁴⁴*Istituto Nazionale di Fisica Nucleare Pisa, ^{bb}University of Pisa, ^{cc}University of Siena and ^{dd}Scuola Normale Superiore, I-56127 Pisa, Italy*
- ⁴⁵*University of Pittsburgh, Pittsburgh, Pennsylvania 15260, USA*
- ⁴⁶*Purdue University, West Lafayette, Indiana 47907, USA*
- ⁴⁷*University of Rochester, Rochester, New York 14627, USA*
- ⁴⁸*The Rockefeller University, New York, New York 10065, USA*
- ⁴⁹*Istituto Nazionale di Fisica Nucleare, Sezione di Roma 1, ^{ee}Sapienza Università di Roma, I-00185 Roma, Italy*
- ⁵⁰*Rutgers University, Piscataway, New Jersey 08855, USA*
- ⁵¹*Texas A&M University, College Station, Texas 77843, USA*
- ⁵²*Texas Tech University, Lubbock, TX 79609, USA*
- ⁵³*Istituto Nazionale di Fisica Nucleare Trieste/Udine, I-34100 Trieste, ^{ff}University of Trieste/Udine, I-33100 Udine, Italy*
- ⁵⁴*University of Tsukuba, Tsukuba, Ibaraki 305, Japan*
- ⁵⁵*Tufts University, Medford, Massachusetts 02155, USA*
- ⁵⁶*University of Virginia, Charlottesville, VA 22906, USA*
- ⁵⁷*Waseda University, Tokyo 169, Japan*
- ⁵⁸*Wayne State University, Detroit, Michigan 48201, USA*
- ⁵⁹*University of Wisconsin, Madison, Wisconsin 53706, USA*
- ⁶⁰*Yale University, New Haven, Connecticut 06520, USA*
- (Dated: November 17, 2021)

A precision measurement of the top quark mass m_t is obtained using a sample of $t\bar{t}$ events from $p\bar{p}$ collisions at the Fermilab Tevatron with the CDF II detector. Selected events require an electron or muon, large missing transverse energy, and exactly four high-energy jets, at least one of which is tagged as coming from a b quark. A likelihood is calculated using a matrix element method with quasi-Monte Carlo integration taking into account finite detector resolution and jet mass effects. The event likelihood is a function of m_t and a parameter Δ_{JES} used to calibrate the jet energy scale *in situ*. Using a total of 1087 events in 5.6 fb^{-1} of integrated luminosity, a value of $m_t = 173.0 \pm 1.2 \text{ GeV}/c^2$ is measured.

PACS numbers: 14.65.Ha

*Deceased

[†]With visitors from ^aUniversity of Massachusetts Amherst, Amherst, Massachusetts 01003, ^bIstituto Nazionale di Fisica Nucleare, Sezione di Cagliari, 09042 Monserrato (Cagliari), Italy, ^cUniversity of California Irvine, Irvine, CA 92697, ^dUniversity of California Santa Barbara, Santa Barbara, CA 93106 ^eUniversity of California Santa Cruz, Santa Cruz, CA 95064, ^fCERN, CH-1211 Geneva, Switzerland, ^gCornell University, Ithaca, NY 14853, ^hUniversity of Cyprus, Nicosia CY-1678, Cyprus, ⁱUniversity College Dublin, Dublin 4, Ireland, ^jUniversity of Fukui, Fukui City, Fukui Prefecture, Japan 910-0017, ^kUniversidad Iberoamericana, Mexico D.F., Mexico, ^lIowa State University, Ames, IA 50011,

^mUniversity of Iowa, Iowa City, IA 52242, ⁿKinki University, Higashi-Osaka City, Japan 577-8502, ^oKansas State University, Manhattan, KS 66506, ^pUniversity of Manchester, Manchester M13 9PL, England, ^qQueen Mary, University of London, London, E1 4NS, England, ^rMuons, Inc., Batavia, IL 60510, ^sNagasaki Institute of Applied Science, Nagasaki, Japan, ^tNational Research Nuclear University, Moscow, Russia, ^uUniversity of Notre Dame, Notre Dame, IN 46556, ^vUniversidad de Oviedo, E-33007 Oviedo, Spain, ^wTexas Tech University, Lubbock, TX 79609, ^xUniversidad Técnica Federico Santa María, 110v Valparaíso, Chile, ^yYarmouk University, Irbid 211-63, Jordan, ^{gg}On leave from J. Stefan Institute, Ljubljana, Slovenia

The top quark is the heaviest known fundamental particle in the standard model of particle physics. Since the 1995 discovery of the top quark at the Fermilab Tevatron [1], both the CDF and D0 experiments have been improving the measurement of its mass m_t , which is a fundamental parameter in the standard model [2]. Loop corrections in electroweak theory relate m_t (along with the W boson mass m_W) to the mass of the predicted Higgs boson. Thus, precision measurements of m_t help to constrain the value of the Higgs boson mass [3].

This Letter describes the single most-precise measurement to date of the top quark mass. It is performed on data collected by the CDF II detector [4] during Run II of the Fermilab Tevatron $p\bar{p}$ collider operating at $\sqrt{s} = 1.96$ TeV with a total integrated luminosity of 5.6 fb^{-1} . The measurement is performed on candidate $t\bar{t}$ events containing a lepton and four jets [5]. For each event selected in this analysis, we calculate the probability of observing that event by integrating the matrix element for $t\bar{t}$ production and decay over phase-space variables. We use a neural network discriminant to distinguish between signal and background events to correct for the contribution due to background, and employ a cut on the peak likelihood for a given event for additional rejection of background and poorly modeled signal events. This analysis offers a gain of nearly 20% in statistical precision over our previous measurement [5] given an equal number of events; there, in order to make the likelihood integration computationally tractable, we introduced kinematic assumptions to reduce the dimensionality of the integral. In the present analysis, we use a quasi-Monte Carlo integration technique [6], which converges more rapidly than the typical $O(N^{-1/2})$ convergence of standard Monte Carlo integration. This allows us to integrate over a total of 19 dimensions in a computationally practical time, resulting in a more accurate modeling of the event. Furthermore, in addition to the increased data sample available with more integrated luminosity delivered by the Tevatron, we have expanded our muon selection ability, which increases the size of our data sample by nearly 30%. In total, this measurement improves our statistical precision by a factor of two over our previous analysis with 1.9 fb^{-1} [5].

In this measurement, the largest uncertainty is due to the uncertainty in the jet energy scale (JES) determination. To reduce this uncertainty, we calculate the likelihood as a two-dimensional function of m_t and a second parameter, Δ_{JES} , which corrects the jet energies by a factor of $1 + \Delta_{\text{JES}} \cdot \sigma_j$, where σ_j is the fractional systematic uncertainty on the energy for a given jet [7, 8]. The known W boson mass is used to constrain the $W \rightarrow q\bar{q}'$ decay, which yields information on the Δ_{JES} parameter. We can thus optimally combine events to reduce the total uncertainty on m_t due to JES.

Within the standard model, the top quark decays al-

most exclusively into a W boson and a b quark. We define a “lepton + jets” event as an event where one of the W bosons produced by the $t\bar{t}$ pair decays into a charged lepton (in this analysis, an electron or a muon) and a neutrino, and the other into a $q\bar{q}'$ pair. The two b quarks and two quarks from the W boson then produce jets in the detector [9]. We thus require candidate events to have an electron with $E_T > 20$ GeV or a muon with $p_T > 20$ GeV/ c in the central detector ($|\eta| < 1$ [10]), or a muon with $p_T > 20$ GeV/ c obtained with a trigger [4] on missing transverse energy, \cancel{E}_T [10], instead of a central muon. As the neutrino energy is not detected, we require $\cancel{E}_T > 20$ GeV in the event. We also require exactly four jets with $E_T > 20$ GeV within the region $|\eta| < 2.0$, at least one of which must be tagged as a b jet using a secondary vertex tagging algorithm [11]. To model $t\bar{t}$ events, we use Monte Carlo-simulated events generated with the PYTHIA [12] generator for 15 different m_t values ranging from 162 to 184 GeV/ c^2 .

Background events contributing to the selected sample are: a) events in which a W boson is produced in conjunction with heavy-flavor quarks ($b\bar{b}$, $c\bar{c}$, or c); b) events in which a W boson is produced along with light quarks, at least one of which is mistagged as heavy flavor; c) QCD events that do not contain a true W boson; d) diboson (WW , WZ , or ZZ) or Z + jets events; e) single top events. We model the contribution from W +jets events using ALPGEN [13], single top events using MADGRAPH [14], and diboson events with PYTHIA. The Z +jets contributions are not modeled separately, but are included in the W +light flavor contribution. All Monte Carlo samples are processed with the CDF II detector response simulation package [15]. The non- W QCD background is modeled using a sideband of data events selected to have a small contribution from heavy boson decay. The numbers of background events are estimated with the method used for the $t\bar{t}$ cross section measurement [16], and are shown in Table I.

For each event, we construct a likelihood as a function of m_t and Δ_{JES} using the following integral:

$$L(\vec{y} | m_t, \Delta_{\text{JES}}) = \frac{1}{N(m_t)} \frac{1}{A(m_t, \Delta_{\text{JES}})} \times \sum_{i=1}^{24} w_i L_i(\vec{y} | m_t, \Delta_{\text{JES}}) \quad (1)$$

$$L_i(\vec{y} | m_t, \Delta_{\text{JES}}) = \int \frac{f(z_1)f(z_2)}{FF} \text{TF}(\vec{y} | \vec{x}, \Delta_{\text{JES}}) \times |M(m_t, \vec{x})|^2 d\Phi(\vec{x}),$$

where \vec{y} are the quantities measured in the detector (the momenta of the jets and charged lepton), \vec{x} are the parton-level quantities that define the kinematics of the event, $N(m_t)$ is a global normalization factor, $A(m_t, \Delta_{\text{JES}})$ is the event acceptance as a function of

TABLE I: Expected sample composition for an integrated luminosity of 5.6 fb^{-1} . The $t\bar{t}$ contribution is estimated using a cross-section of 7.4 pb [17] and $m_t = 172.5 \text{ GeV}/c^2$.

Event type	1 b tag	≥ 2 b tags
W +heavy flavor	129.5 ± 42.1	15.7 ± 5.5
non- W QCD	50.1 ± 25.5	5.5 ± 3.8
W +light flavor mistag	48.5 ± 17.1	1.0 ± 0.4
diboson (WW, WZ, ZZ)	10.5 ± 1.1	1.0 ± 0.1
Single top	13.3 ± 0.9	4.0 ± 0.4
$Z \rightarrow \ell\ell$ + jets	9.9 ± 1.2	0.8 ± 0.1
Total background	261.8 ± 60.6	28.0 ± 9.6
$t\bar{t}$ signal	767.3 ± 97.2	276.5 ± 43.0
Total expected	1029.1 ± 114.5	304.5 ± 44.1
Events observed	1016	247

m_t and Δ_{JES} , $f(z_1)$ and $f(z_2)$ are the parton distribution functions (PDFs) for incoming parton momentum fractions z_1 and z_2 , FF is the relativistic flux factor, $\text{TF}(\vec{y} | \vec{x}, \Delta_{\text{JES}})$ are the transfer functions that describe the measured jet-momentum distributions given the quark kinematics, $d\Phi(\vec{x})$ the phase space for the eight particles in the $t\bar{t}$ production and decay process, and $M(m_t, \vec{x})$ is the matrix element for the process. The integral is calculated for each of the 24 possible permutations of jet-parton assignment and then summed with weights w_i determined by the probability that a b or light parton will result in a b -tagged or untagged jet.

We use the Kleiss-Stirling matrix element [18], which is a leading-order matrix element including both $q\bar{q} \rightarrow t\bar{t}$ and $gq \rightarrow t\bar{t}$ production processes, as well as all spin correlations. For the PDFs, we use the CTEQ5L functions [19] for the incoming $q\bar{q}$ and gluons. The normalization factor $N(m_t)$ is obtained by integrating the Kleiss-Stirling matrix element with the PDFs and the flux factor over the phase space formed by the two initial and the six final-state particles. The acceptance $A(m_t, \Delta_{\text{JES}})$ is obtained from simulated events where the parton directions and momenta are smeared to simulate final-state jets. The transfer functions connect the measured jets to the partons. We construct the transfer functions by taking simulated $t\bar{t} \rightarrow \text{lepton} + \text{jets}$ events in a wide range of masses and matching the simulated jets to their parent partons. The transfer functions are separated into momentum and angular terms; both are constructed with dependence on the true jet p_T and mass from the Monte Carlo simulation. The transfer functions are constructed separately for b and light quarks, as well as for each of four bins of jet η . There are 32 phase space integration variables in Eq. (1) (for the two initial partons and six final partons). Four of these are eliminated by energy and momentum conservation, and four more by taking the charged lepton, neutrino, and initial parton masses

as known. In addition, we assume that the lepton momentum is perfectly measured, and we neglect the effects of the individual transverse momenta of the initial partons so that we model only the transverse momentum of the total $t\bar{t}$ system, for which we use a prior derived from Monte Carlo simulation. This leaves a total of 19 dimensions over which the integral must be evaluated, which we perform using a quasi-Monte Carlo technique.

Handling of background events is unchanged from our previous publication [5]. We identify events likely to be background using a JETNET 3.5 artificial neural network [20] with ten inputs. We construct distributions of the neural network output weight u for signal, $S(u)$, and background, $B(u)$, events, normalized to their overall expected fractions, and calculate the expected background fraction for a given event as $f_{\text{bg}}(u) = B(u)/(B(u) + S(u))$.

We calculate the likelihood for all candidate events under the assumption that they are signal, but the combined likelihood contains contributions from both signal and background events. However, only the signal events contain information about m_t , so using Monte Carlo-simulated events we compute the average likelihood for background events and subtract it from the total likelihood:

$$\begin{aligned} & \log L_{\text{adj}}(m_t, \Delta_{\text{JES}}) \\ &= \sum_{i \in \text{Events}} [\log L(\vec{y}_i | m_t, \Delta_{\text{JES}}) - f_{\text{bg}}(u_i) \log \overline{L}_{\text{bg}}(m_t, \Delta_{\text{JES}})], \end{aligned} \quad (2)$$

where L_{adj} is the adjusted total likelihood for a given set of events, $L(\vec{y}_i | m_t, \Delta_{\text{JES}})$ is the likelihood for an individual event from Eq. (1), $f_{\text{bg}}(u_i)$ is the background fraction for a given event with a neural network output u_i , and $\overline{L}_{\text{bg}}(m_t, \Delta_{\text{JES}})$ is the average likelihood for a background event.

Besides background events, the sample includes events which contain a real $t\bar{t}$, but where one or more of the four jets and/or the lepton observed in the detector do not come directly from the $t\bar{t}$ decay, and are not well-modeled by the signal likelihood or handled by the background subtraction above. These events, which we refer to as “bad signal,” have a variety of sources (extra jets from gluon radiation, $t\bar{t}$ events where both W bosons decay into leptons or hadrons, $W \rightarrow \tau\nu$ decay, etc.) and make up 36% of the simulated $t\bar{t}$ events for $m_t = 172.5 \text{ GeV}/c^2$. We suppress these events by requiring that the peak log-likelihood value for an event be at least 10. This cut retains 96.3% of the signal, while rejecting 30.8% of the bad signal and 37.3% of the background.

We test and calibrate the method by constructing simulated experiments using the Monte Carlo samples of $t\bar{t}$ events and background described earlier. For a given input m_t and Δ_{JES} , we perform 2000 experiments using a Poisson distribution with mean of 1089 events (the num-

ber of events expected to pass the likelihood cut), and use these to calibrate the measurement as a function of the input m_t and Δ_{JES} . Figure 1 shows the output mass before calibration and the calibrated expected uncertainty.

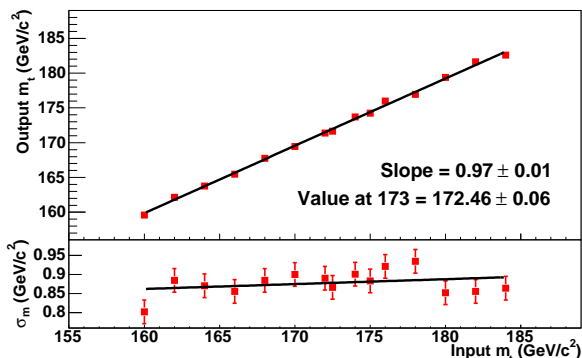


FIG. 1: Simulated experiment results using Monte Carlo signal and background events. Top: output m_t vs. input m_t , before calibration is applied. Bottom: expected uncertainty σ_m vs. input m_t , with calibration applied. The lines are linear best fits.

In the data we find a total of 1087 events which pass all of the selection requirements (including the likelihood peak cut), of which 854 have 1 b tag and 233 have >1 b tag. Figure 2 shows the resulting 2-D likelihood contours for 1 σ , 2 σ , and 3 σ after all calibration.

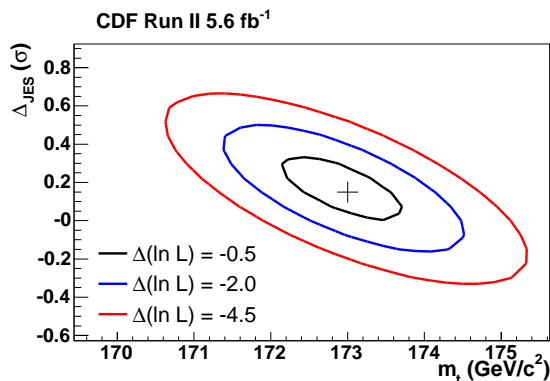


FIG. 2: Measured 2-D likelihood on the data events, with the contours corresponding to a 1- σ , 2- σ , and 3- σ uncertainty in the final m_t measurement from the profile method. The marker shows the point of maximum likelihood.

To obtain a 1-D likelihood curve in m_t only, we treat Δ_{JES} as a nuisance parameter and eliminate it using the profile likelihood method [21], where we take the maximum value of the likelihood along the Δ_{JES} axis for each m_t value. The top quark mass value extracted from the profile likelihood after calibration is $m_t = 173.0 \pm 0.9$ GeV/c^2 . We can separate this uncertainty into the statistical uncertainty on m_t and the uncertainty due to

Δ_{JES} by fixing the Δ_{JES} value to its maximum likelihood value. We find that the uncertainty from the resulting 1-D likelihood is 0.7 GeV/c^2 , so we assign the remaining uncertainty of 0.6 GeV/c^2 to Δ_{JES} and conclude $m_t = 173.0 \pm 0.7$ (stat.) ± 0.6 (JES) GeV/c^2 .

To validate the likelihood cut procedure, we compare the peak values of the log-likelihood curves obtained with data to those obtained with Monte Carlo-simulated events at $m_t = 172.5$ GeV/c^2 (the nearest available mass value). The results are shown in Fig. 3.

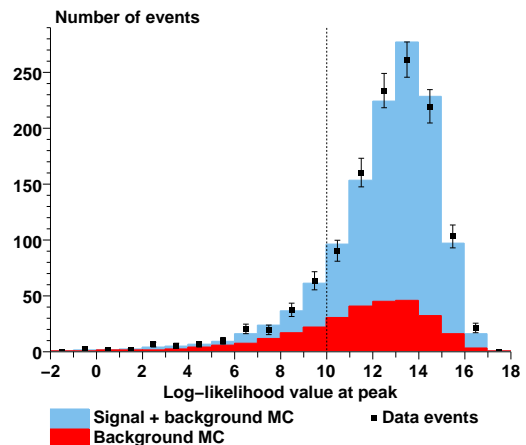


FIG. 3: Comparison of the log-likelihood value of the peak of likelihood curves for data and Monte Carlo events. The vertical line at 10 indicates the likelihood cut used in this analysis. A Kolmogorov-Smirnov test gives a confidence level of 0.93, showing good agreement between the two.

The systematic uncertainties on m_t , given in Table II, are derived using the methods described in Ref. [5]. In brief, we include uncertainties coming from: the calibration method; signal Monte Carlo modeling, evaluated by comparing events simulated with the PYTHIA and HERWIG [22] generators; variations of the parameters used for initial state radiation (ISR) and final state radiation (FSR); a residual JES uncertainty because the JES uncertainty contains several components with different p_T and η dependence; additional uncertainties on the energy scale for b jets; uncertainty on the lepton p_T scale; multiple hadron interactions, to take into account uncertainty on the jet corrections as a function of the number of interactions in the event; uncertainties arising from the PDFs used in the integration; and the background modeling. This analysis includes a systematic uncertainty due to color reconnection effects, not considered in our previous analysis. We use PYTHIA version 6.4.20, which includes a color reconnection model [23], and measure the difference between two tunes, Tune A, which is the tune used in this analysis, and Tune ACR, which adds color reconnection effects to Tune A. The individual systematic uncertainties are added in quadrature to obtain the final total of 0.9 GeV/c^2 .

In conclusion, the measured top quark mass in a sample with 5.6 fb^{-1} of integrated luminosity, with 1087 events passing all cuts, is $m_t = 173.0 \pm 0.7 \text{ (stat.)} \pm 0.6 \text{ (JES)} \pm 0.9 \text{ (syst.) GeV}/c^2$, for a total uncertainty of $1.2 \text{ GeV}/c^2$. The improved integration techniques and increased data sample make this the best single measurement of the top quark mass to date, and it is comparable in precision to the most recent combination for the top quark mass at the Tevatron [2].

We thank the Fermilab staff and the technical staffs of the participating institutions for their vital contributions. This work was supported by the U.S. Department of Energy and National Science Foundation; the Italian Istituto Nazionale di Fisica Nucleare; the Ministry of Education, Culture, Sports, Science and Technology of Japan; the Natural Sciences and Engineering Research Council of Canada; the National Science Council of the Republic of China; the Swiss National Science Foundation; the A.P. Sloan Foundation; the Bundesministerium für Bildung und Forschung, Germany; the World Class University Program, the National Research Foundation of Korea; the Science and Technology Facilities Council and the Royal Society, UK; the Institut National de Physique Nucleaire et Physique des Particules/CNRS; the Russian Foundation for Basic Research; the Ministerio de Ciencia e Innovación, and Programa Consolider-Ingenio 2010, Spain; the Slovak R&D Agency; and the Academy of Finland.

-
- [1] F. Abe *et al.* (CDF Collaboration), Phys. Rev Lett. **74**, 2626 (1995); S. Abachi *et al.* (D0 Collaboration), *ibid.* **74**, 2632 (1995).
 [2] The Tevatron Electroweak Working Group, FERMILAB-TM-2466-E, arXiv:1007.3178v1 (2010).
 [3] The LEP Collaboration, CERN-PH-EP/2007-039,

arXiv:0712.0929v2.

- [4] D. Acosta *et al.* (CDF Collaboration), Phys. Rev. D **72**, 052003 (2005).
 [5] T. Aaltonen *et al.* (CDF Collaboration), Phys. Rev. D **79**, 072001 (2009).
 [6] W. Morokoff and R. E. Caflisch, SIAM J. Sci. Stat. Comp. **15**, 1251 (1994).
 [7] A. Abulencia *et al.* (CDF Collaboration), Phys. Rev. Lett. **96**, 022004 (2006).
 [8] A. Bhatti *et al.* (CDF Collaboration), Nucl. Instrum. Meth. A **566**, 375 (2006).
 [9] F. Abe *et al.* (CDF Collaboration), Phys. Rev. D **45**, 1448 (1992).
 [10] A particle's transverse momentum p_T and transverse energy E_T are given by $|\vec{p}|\sin\theta$ and $E\sin\theta$ respectively, where θ is the polar angle with respect to the proton direction (z -axis). The pseudorapidity η of a particle's three-momentum is defined by $\eta = -\ln(\tan(\theta/2))$. The missing E_T , \cancel{E}_T , is defined by $\vec{\cancel{E}}_T = -|\sum_i E_{T_i} \hat{n}_{T_i}|$, where \hat{n}_{T_i} is the unit vector in the x - y plane pointing from the primary vertex to a given calorimeter tower i , and E_{T_i} is the E_T measured in that tower.
 [11] D. Acosta *et al.* (CDF Collaboration), Phys. Rev. D **71**, 052003 (2005).
 [12] T. Sjöstrand *et al.*, Comput. Phys. Commun. **135**, 238 (2001).
 [13] M. Mangano *et al.*, J. High Energy Phys. **07**, 001 (2003).
 [14] F. Maltoni and T. Stelzer, J. High Energy Phys. **02**, 027 (2003).
 [15] E. Gerchtein, M. Paulini, arXiv:physics/0306031 (2003).
 [16] D. Acosta *et al.* (CDF Collaboration), Phys. Rev. D **71**, 072005 (2005).
 [17] S. Moch and P. Uwer, Nucl. Phys. Proc. Suppl. **183**, 75 (2008).
 [18] R. Kleiss and W. J. Stirling, Z. Phys. C **40**, 419 (1988).
 [19] H. L. Lai *et al.*, Eur. Phys. J. C **12**, 375 (2000).
 [20] C. Peterson, T. Rognvaldsson, and L. Lönnblad, Comput. Phys. Commun. **81**, 185 (1994).
 [21] G. A. Young and R. L. Smith, *Essentials of Statistical Inference* (Cambridge University Press, 2005).
 [22] G. Corcella *et al.*, J. High Energy Phys. **01**, 010 (2001).
 [23] P. Skands and D. Wicke, Eur. Phys. J. C **52**, 1 (2007).

TABLE II: List of systematic uncertainties on m_t .

Systematic source	Uncertainty (GeV/c^2)
Calibration	0.10
MC generator	0.37
ISR and FSR	0.15
Residual JES	0.49
b -JES	0.26
Lepton p_T	0.14
Multiple hadron interactions	0.10
PDFs	0.14
Background modeling	0.33
Color reconnection	0.37
Total	0.88